Received: 22 September 2017 | Revised: 2 May 2018 | Accepted: 20 May 2018

DOI: 10.1111/bre.12301

ORIGINAL ARTICLE

WILEY Basin Research IAS EAGE

Evolution of the central West Greenland margin and the Nuussuaq Basin: Localised basin uplift along a stable continental margin proposed from thermochronological data

Scott Jess[1] | **Randell Stephenson**[1] | **Roderick Brown**[2]

[1]School of Geosciences, University of Aberdeen, Aberdeen, UK

[2]School of Geographical and Earth Sciences, University of Glasgow, Glasgow, UK

Correspondence
Scott Jess, School of Geosciences, University of Aberdeen, Aberdeen, UK.
Email: r01sj14@abdn.ac.uk

Abstract

The Late Cenozoic is typically considered a time of widespread episodic tectonic uplift along the West Greenland continental margin (36–2 Ma), similar to other margins across the North Atlantic, such as Norway, East Greenland and the UK. The present study re-examines and remodels onshore thermochronological data from central West Greenland and the Cretaceous Nuussuaq Basin, utilising a Bayesian modelling approach and new concepts related to radiation damage within apatite. These new thermal histories indicate that slow-protracted cooling has occurred across the southern extent of the margin during the Mesozoic and Cenozoic, whereas those from within the Nuussuaq Basin display reheating through the Late Cretaceous/Palaeogene and cooling to present. Results suggest that no significant Late Cenozoic uplift has occurred along the southern margin, while cooling in the Nuussuaq Basin is consistent with events outlined in the basin's stratigraphy and implies uplift during volcanism and an isostatic response to the unroofing of the lithosphere has elevated the modern topography. These results imply significant tectonism in the region ceased by ~45 Ma, yet have wider implications regarding how low temperature thermochronology data are treated and our understanding of the postrift evolution of passive margins.

KEYWORDS

modelling, passive margins, stratigraphy, tectonics and sedimentation, thermochronology

1 | INTRODUCTION

A number of rifted continental margins across the globe exhibit elevated coastal topography, complex sedimentary geometries and widespread volcanism implying continued tectonic activity in their 'post-rift' stages (e.g. Chalmers, 2000; Eidvin, Riis, & Rasmussen, 2014; Hansen, 1996; Japsen, Green, & Chalmers, 2005; Riis, 1996; Rohrman & van der Beek, 1996), yet an underlying cause for tectonic rejuvenation is rarely evident. Onshore Cenozoic geology is seldom preserved; therefore, low temperature thermochronology has been widely employed to ascertain thermal histories, used to infer the denudational history of the landscape (Hendriks & Andriessen, 2002; Johannessen, Kohlmann, Ksienzyk, Dunkl, & Jacobs, 2013; Johnson & Gallagher, 2000; Wildman et al., 2015). This approach has been successful in establishing key elements of passive margin development, outlining onshore denudational patterns and reactivation of major fault zones (Gallagher & Brown, 1997), although it has also provided

a range of contentious conclusions as to whether margin topography is derived from tectonics or denudation (Brown & Green, 1991; Chalmers, Green, Japsen, & Rasmussen, 2010; Green, 1989; Nielsen et al., 2009; Redfield, 2010).

The West Greenland margin is a Mesozoic rift flank in the Northern Atlantic underlain by Archaean/Proterozoic basement and composed of mountainous coastal topography, an elevated onshore Cretaceous/Palaeocene basin (the Nuussuaq Basin) and widespread Palaeogene basaltic volcanism. Late Cenozoic tectonically induced uplift of ~3 km is widely believed to have shaped the modern landscape (e.g. Alsulami, Paton, & Cornwell, 2015; Dalhoff et al., 2003; Dam et al., 2009; Gregersen, Hopper, & Knutz, 2013), based on the modelling of low temperature thermochronological data and geomorphological analysis of the margins topography (Japsen, Bonow, Green, Chalmers, & Lidmar-Bergström, 2006). Thermal histories derived from fission track (AFT), apatite (U-Th)/He (AHe) and vitrinite reflectance (VR) data from five wells within the Nuussuaq Basin (Figure 1) have been interpreted as evidence for three significant cooling episodes (36–30 Ma, 11–10 Ma and 7–2 Ma; Figure 2) corresponding with tilted unconformities offshore (Chalmers, 2000) and elevated 'peneplains' onshore (Green, Moore, O'Brien, & Crowhurst, 2003c; Japsen et al., 2006). This interpretation was challenged by Redfield (2010), who highlighted the aspects of the treatment of the data and of the thermal modelling approach and proposed a conceptual model invoking heterogeneous flexural isostatic response to erosional unloading onshore and sediment deposition offshore (cf. fig. 5c from Redfield et al., 2005). Redfield's (2010) interpretations were based on AFT age trends across the margin and not thermal modelling due to perceived data insufficiencies for thermal modelling.

The present work applies a Bayesian modelling approach to the West Greenland data set that incorporate the data uncertainties into the modelling methodology itself (Gallagher, 2012). The approach taken enables the joint inversion of all data for a given sample, modelling of multiple samples from elevation profiles or wells and accommodates radiation damage within apatite (Flowers, Ketcham, Shuster, & Farley, 2009; Gautheron, Tassan-Got, Barbarand, & Pagel, 2009). The well-documented stratigraphy of the Nuussuaq basin allows for better constrained thermal models and provides critical information regarding the basin's evolution that assists in the interpretation of thermal histories. Newly generated thermal histories outline an onshore history of the West Greenland Margin consistent with regional geological observations, though they also raise questions about the interpretation of the thermochronological data and the extent of tectonic rejuvenation along passive continental margins.

Highlights

- Our results strengthen arguments against late Cenozoic (postrift) tectonism being responsible for the present-day elevated topography on the west Greenland margin.
- These results have implications for continental margin geomorphology, in general, across the North Atlantic realm.
- This work highlights how a Bayesian modelling approach can help with the interpretation of complex data sets.

2 | GEOLOGICAL SETTING

The basement of Western Greenland is composed of Archaean/Proterozoic orthogneiss and banded gneiss formed prior to and during the Trans-Hudson Orogeny (1.8 Ga; St-Onge, van Gool, Garde, & Scott, 2009). Lithospheric extension from the Late Triassic to the Early Palaeocene (~228–64 Ma) formed the present-day rifted margins of Baffin Bay and the onshore Nuussuaq Basin, both of which incorporate Cretaceous and Palaeocene stratigraphy (Figure 3; Chalmers, Pulvertaft, Marcussen, & Pedersen, 1999; Dam et al., 2009). Sea-floor spreading in Baffin Bay is thought to have replaced rifting in the Late Palaeocene and was kinematically reorientated (N-S to NNW-SSE) between the Late Palaeocene and Early Eocene (~57–53 Ma) before terminating in the late Eocene (~34 Ma; Oakey & Chalmers, 2012).

The Nuussuaq Basin's clastic stratigraphy comprises mass flow, fluvial and lacustrine deposits from the Mid-Cretaceous; deltaic, estuarine and fluvial deposits from the Mid to Late Cretaceous; and deep marine mudstones from the Late Cretaceous (Figure 3). The deltaic Atane Formation covers much of the southern, central and eastern parts of the basin and, in the west, is overlain by deep marine mudstones and turbidite sands of the Itilli Formation, representing a transition from delta front to shelf slope. Extensional tectonism in the Late Cretaceous is inferred from the formation of a deep submarine canyon fill (Kangilia Formation) and is followed by uplift and rapid subsidence in the Early Palaeocene represented by incised valleys onshore (Quikavsak Formation) and further submarine canyons offshore (Agatdal Formations) (Dam & Nøhr-Hansen, 2001; Figure 3). Folding of the Itilli Formation perpendicular to the Itilli Fault plane (Figure 1; Chalmers et al., 1999) is evidence of localised compression in the basin, though the timing and cause of deformation is difficult to constrain as the Mesozoic fault is likely to have been reactivated in the Palaeocene and Eocene (Abdelmalak et al., 2012).

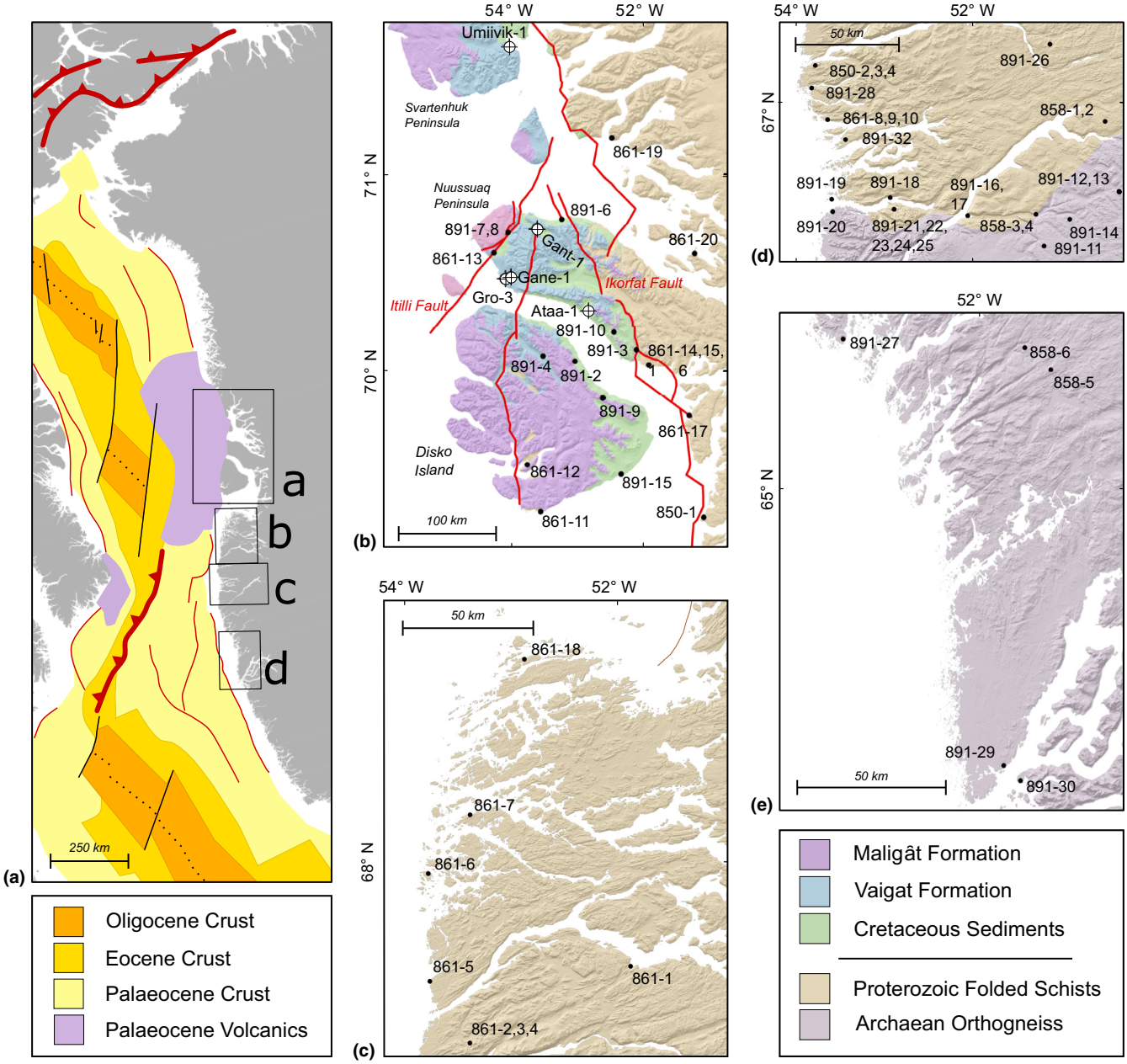

FIGURE 1 Simplified regional geology and sample locations of the West Greenland data set from outcrop and wells (Green, Moore, Gibson, & O'Brien, 2004; Green, Moore, O'Brien, & Crowhurst, 2003a,b; Green et al., 2002, 2003c). The regional geological map (a) outlines the major structural features, offshore geology and the location of each region along central West Greenland: adapted from Oakey and Chalmers (2012). Samples are split into four separate regions: b) Nuussuaq, c) Aasiaat, d) Sisimiut and e) Nuuk and wells from within the Nuussuaq Basin can be found in the Data S1

Volcanism in the Palaeogene dramatically altered the basin's evolution, depositing submarine volcaniclastics and picrites in the Early Palaeocene and flood basalts from the Mid-Palaeocene to the Late Eocene (~61 Ma – ~38 Ma; Figure 3). Volcaniclastics of the Eqalulik Formation are observed west of the Ikorfat Fault (Figure 1) and are composed of sandy turbidites and tuffaceous mudstones underlying the pillow breccias and hyaloclastites of the lower Vaigat Formation. The subaerial picrite lavas of the upper Vaigat Formation continue further east across the basin and are later overlain by the flood basalts of the Maligât Formation, observed over much of the central margin and damming the basin in the Palaeocene forming the lacustrine deposits of the Atanikerluk Formation (Dam et al., 2009). Volcanism continued until the Late Eocene covering much of the margin with the basalts of the Svartenhuk and Naqerloq formations and emplacing dykes and sills within Cretaceous successions (Larsen et al., 2016) (Figure 3). Intra-volcanic sedimentary sequences are observable within the volcanic succession and demonstrate that early

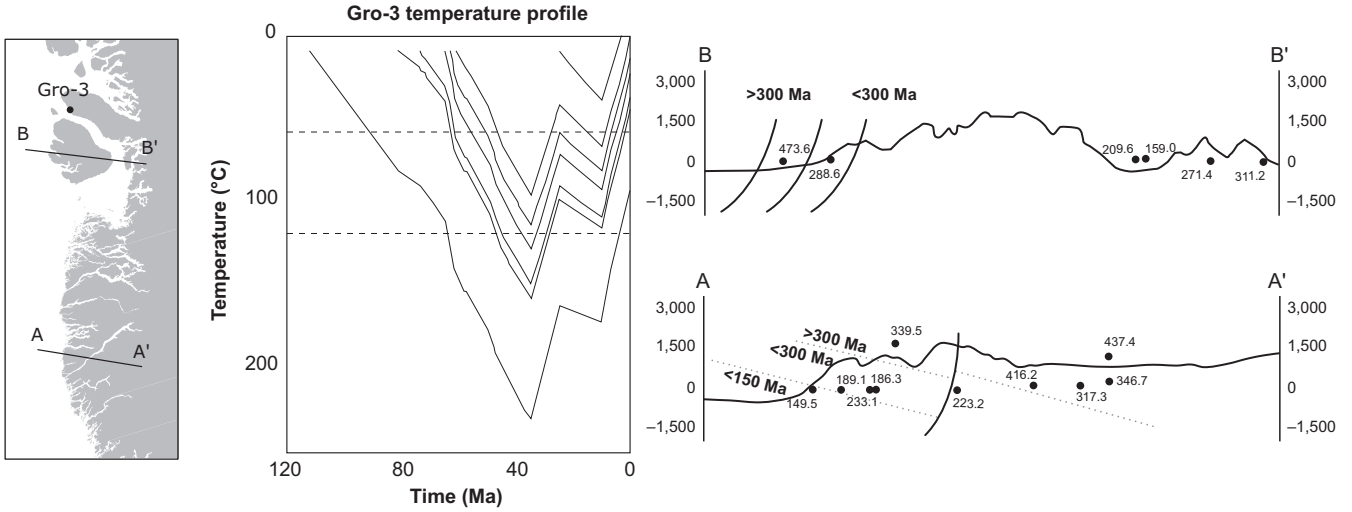

FIGURE 2 Two previous interpretations of the West Greenland Margin data set. The Gro-3 temperature profile exhibits reheating from ~110 Ma to ~35 Ma followed by two pronounced periods of cooling (~35–25 Ma; 10–0 Ma) taken from Green et al. (2003c). Cooling events outlined here are coupled to 'peneplain' surfaces across the margin's topography, concluding that up to 3 km of tectonic uplift has occurred in the Neogene (Japsen et al., 2006). Spatial trends of AFT ages across the margin suggest a faulted rift flank formed in the Mesozoic, outlined in two cross sections (A-A'; B-B') taken from Redfield (2010). This interpretation implies a heterogeneous flexural isostatic response to erosional unloading onshore and sediment deposition offshore has created the age trends we see

volcanism (Vaigat Formation) was marine in the west and subaerial in the east, while later stages (Maligât Formation) remained as subaerial until a marine transgression in the Mid-Palaeocene (Dam et al., 2009; Piasecki, Larsen, Pedersen, & Pedersen, 1992).

3 | DATA & METHODOLOGY

3.1 | West Greenland dataset

The data used in this study are the supplementary data of Japsen et al. (2006) and consist of 63 vitrinite reflectance values, 77 AFT analyses and 166 AHe single grain ages (data tables can be found within the Data S1). The data from the margin are initially assessed in groups from four separate regions (Nuussuaq, Aasiaat, Sisimiut and Nuuk; Figure 1) to establish the regional thermal history of each before integrating them to produce a margin wide interpretation. Table 1 summarises the AFT and AHe data for each region and the VR data for all five wells across the Nuussuaq Basin. Characteristics of the data set include:

1 Thirty-two AFT samples that contain less than the minimum recommended ~100 track lengths considered necessary for effectively constraining thermal models (Donelick, O'Sullivan, & Ketcham, 2005) and suggest that the track length distribution is not wholly represented. Although these samples do not contain the desired number of track lengths, they still retain valuable thermal history information that may be utilised in a Bayesian approach and correlated with other AFT, AHe and VR data in a joint inversion. Consistently poor data, in contrast, will be reflected by the 95% confidence bounds in the produced thermal history.
2 Radiation-enhanced annealing within the basement AFT samples was outlined as a possible control on the ages across the West Greenland margin by Redfield (2010) and is thought to produce younger AFT single grain ages with higher uranium concentrations (Hendriks & Redfield, 2005). Although 15 of the 50 AFT samples show a weak to moderate positive correlations between uranium content and single grain age, the cause of this effect is the subject of a contentious debate within the literature given its absence in similar data sets and the reliability of the negative correlation (Kohn et al., 2009; Larson, Cederbom, Tullborg, & Stiberg, 2006). Moreover, single grain age error can be significant (≤50%) and further correlates to the uranium content of each grain, likely sourced from a lower number of fission tracks in grains with lower uranium content, increasing the calculated error, suggesting that these negative trends may be inaccurate. These contentions suggest that the possible effect of radiation damage on the AFT ages is unlikely and as such will not be explored further within this work.
3 Single grain AHe ages from basement lithologies display high levels of age dispersion ranging between 4% and 225%. Dispersion of the AHe ages can be attributed to several possible factors; ^{4}He ejection (Farley, Wolf, & Silver, 1996), ^{4}He implantation (Spiegel, Kohn, Belton, Berner, & Gleadow, 2009), U- and Th-

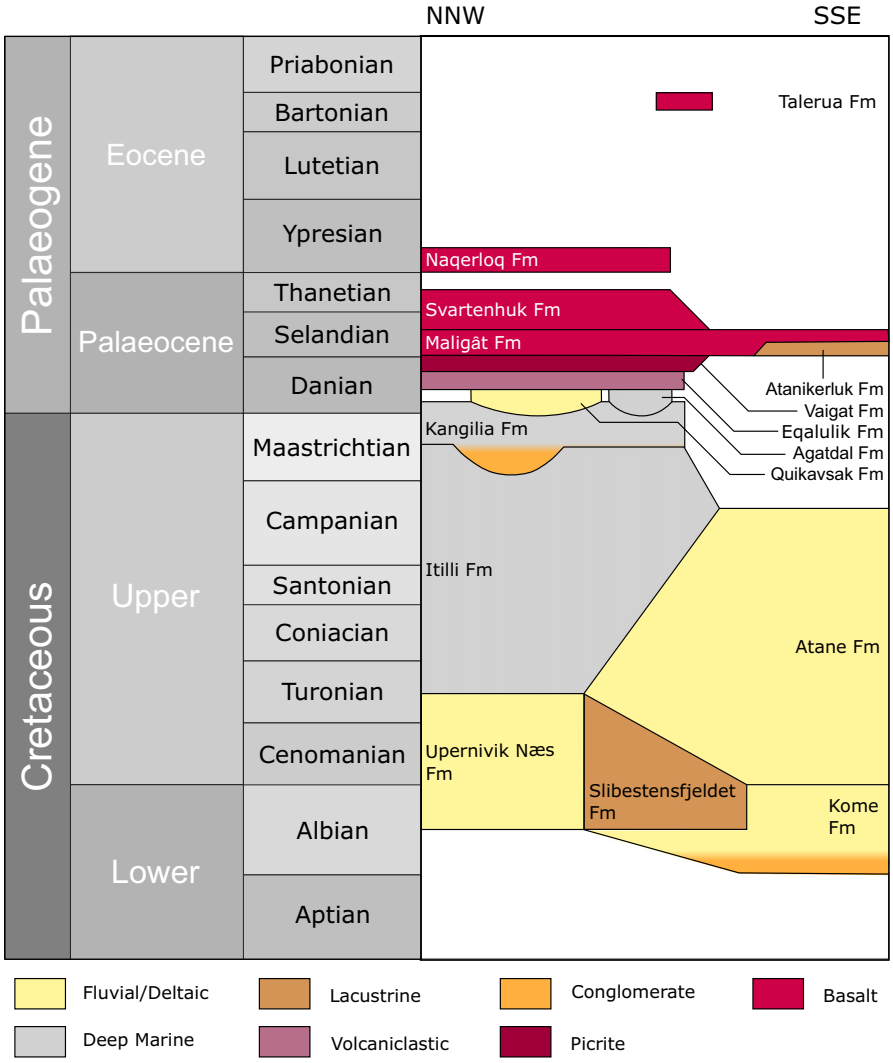

FIGURE 3 Simplified chronostratigraphy of the Nuussuaq Basin adapted from Dam et al. (2009), Gregersen et al. (2013) and Larsen et al. (2016). Deltaic and lacustrine deposits dominate early sedimentation as they infill the palaeotopography of the underlying basement and are later overlain by the major deltaic sequences of the Atane Formation in the SE and the deep marine mudstones and turbidites of the Itilli Formation to the NW. Extension and uplift in the Late Cretaceous lead to the deposition of the Kangilia, Quikavsak and Agatdal formations prior to the onset of Palaeogene volcanism. Volcanism lasted into the Early Eocene as the submarine and subaerial picrites and basalts of the Vaigat, Maligât, Svartenhuk and Naqerloq formations covered much of the onshore and offshore

TABLE 1 General summary of the data presented in Green et al. (2002, 2003a,b,c, 2004). AFT and AHe data are split into the four regions of central West Greenland and range VR data for each well from the Nuussuaq Basin is provided. A full AFT and AHe data table are found within the Data S1

Region	AFT ages (Ma)	MTL (μm)	AHe age (Ma)	Well	VR (%Ro)
Nuussuaq				Gro-3	0.77–2.29
Sedimentary	20.5 ± 5.4–355.8 ± 20.9	8.8 ± 0.62–13.4 ± 0.66	0.29 ± 0.29–211.48 ± 7.04	Ataa-1	0.50–0.57
Basement	159.0 ± 14.0–473.6 ± 30.1	11.77 ± 1.99–13.34 ± 3.04	46.56 ± 5.66–607.91 ± 70.66	Gane-1	0.58–0.75
Aasiaat	175.2 ± 9.1–403 ± 30.5	12.31 ± 2.17–13.24 ± 1.98	93.59 ± 10.6–480.55 ± 53.97	Gant-1	0.63–1.13
Sisimiut	149.5 ± 10.8–437.4 ± 24.1	12.03 ± 2.18–13.33 ± 2.06	93 ± 2.95–3965.31 ± 213.24	Umiivik-1	0.55–4.31
Nuuk	112.8 ± 7.2–231.5 ± 15.5	11.54 ± 2.31–13.81 ± 1.54	71.81 ± 2.21–973.31 ± 35.61		

rich mineral inclusions (Fitzgerald, Baldwin, Webb, & O'Sullivan, 2006; Vermeesch et al., 2007), zonation (Flowers & Kelley, 2011), fragmentation (Brown et al., 2013), grain size (Reiners & Farley, 2001) and radiation damage (Djimbi et al., 2015; Flowers et al., 2009; Gautheron et al., 2009, 2013; Gerin et al., 2017; Shuster, Flowers, & Farley, 2006), all of which can augment the age and increase the level of age dispersion. In roughly half of the samples, AHe age exhibits a weak to moderate positive trend against eU, while only 4 of 28 samples exhibit a weak to moderate positive correlation between AHe age and equivalent radius (Figure 4 and Data S1). This implies that radiation damage may be a significant cause of age dispersion (Flowers et al., 2009), though the limited number of ages per sample should be noted.

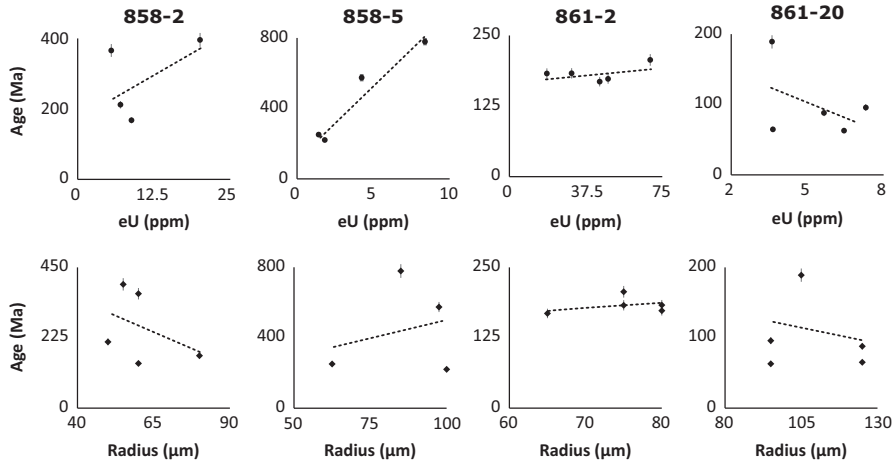

FIGURE 4 Plots of AHe age against [eU] and equivalent grain radius from four samples across the West Greenland Margin, indicative of the wider data set. [eU] plots consistently show a weak to moderate positive correlation (except from 861 to 20) suggesting the effect of radiation damage on the samples may be significant, while radius trends show a variation of positive and negative trends. The variation in these parameters can make it difficult to ascertain robust correlations within samples as the AHe age itself is a combination eU, radius and thermal history

4 All VR data from wells in the Nuussuaq Basin imply a higher geothermal gradient than that at present, while data from the Umiivik-1 well show peaks in %Ro at various depths that do not define a simple stratigraphically driven thermal history, implying the localised heating of sediments by igneous intrusions (Green et al., 2003c) and reducing the number of usable VR data points. The use of the Bayesian-modelling approach allows for a variable geothermal gradient through time and can also choose to reject VR data that have been overprinted if it fails to relate to the AFT and AHe data in the well, objectively removing it.

5 11 sedimentary samples from the southern extent of the Nuussuaq Basin and atop fault zones include central ages older than the estimated stratigraphic age, indicating that sufficient annealing of provenance tracks has not occurred. This is likely due to either limited burial of these locations or compositional heterogeneity and implies that postdepositional thermal histories are unlikely to be generated.

6 Grain ages from samples in the Gro-3 well show a wide range of values uncorrelated to the Cl wt% suggesting contamination during the drilling, meaning thermal history information from these samples may be compromised (Green et al., 2003c). Moreover, the number of track lengths measured from the well ranges between 4 and 16 per sample, implying the narrow track distributions provided are poor representations of the whole population, further hindering any thermal modelling of the samples. Although a different modelling approach may produce a thermal history consistent with the measured data, the results will be treated with care and likely have little interpretive value.

In the present work, an integrated Bayesian approach is used to take account of the complex and variable quality of the data in fitting thermal histories to the observed data, assisting in interpretation and allowing for the use of a greater number of the AHe ages as additional constraints.

3.2 | Inverse modelling

The modelling approach employed in this work uses the QTQt software, incorporating a Bayesian transdimensional Markov Chain Monte Carlo (MCMC) inversion technique (Gallagher, 2012). This method iterates $\geq 10^6$ thermal histories within a set model space assessing the probability of success for each against the measured data to generate an 'expected model' of the sample's history (based on a weighted average of the probability distribution). AFT, VR and AHe data from a single sample are jointly modelled and constrain a single, common thermal history, while multiple samples from varying elevations may also be modelled together to constrain a common thermal history applicable to an elevation profile or well. This approach accounts for and, accordingly, demonstrates the quality of the available data and addresses uncertainties within models and modelling parameters due to its reliance on a distribution of numerous probable forward histories.

Dispersion in the AHe data set can make it difficult to produce accurate age predictions jointly modelled with AFT data. The inclusion of a radiation damage model within QTQt and diffusion parameters and resampling the AHe age error improves modelling results given the ranges of age dispersion and eU concentrations, while providing an objective mechanism for identifying individual grain ages that are incompatible (within analytical error) with the

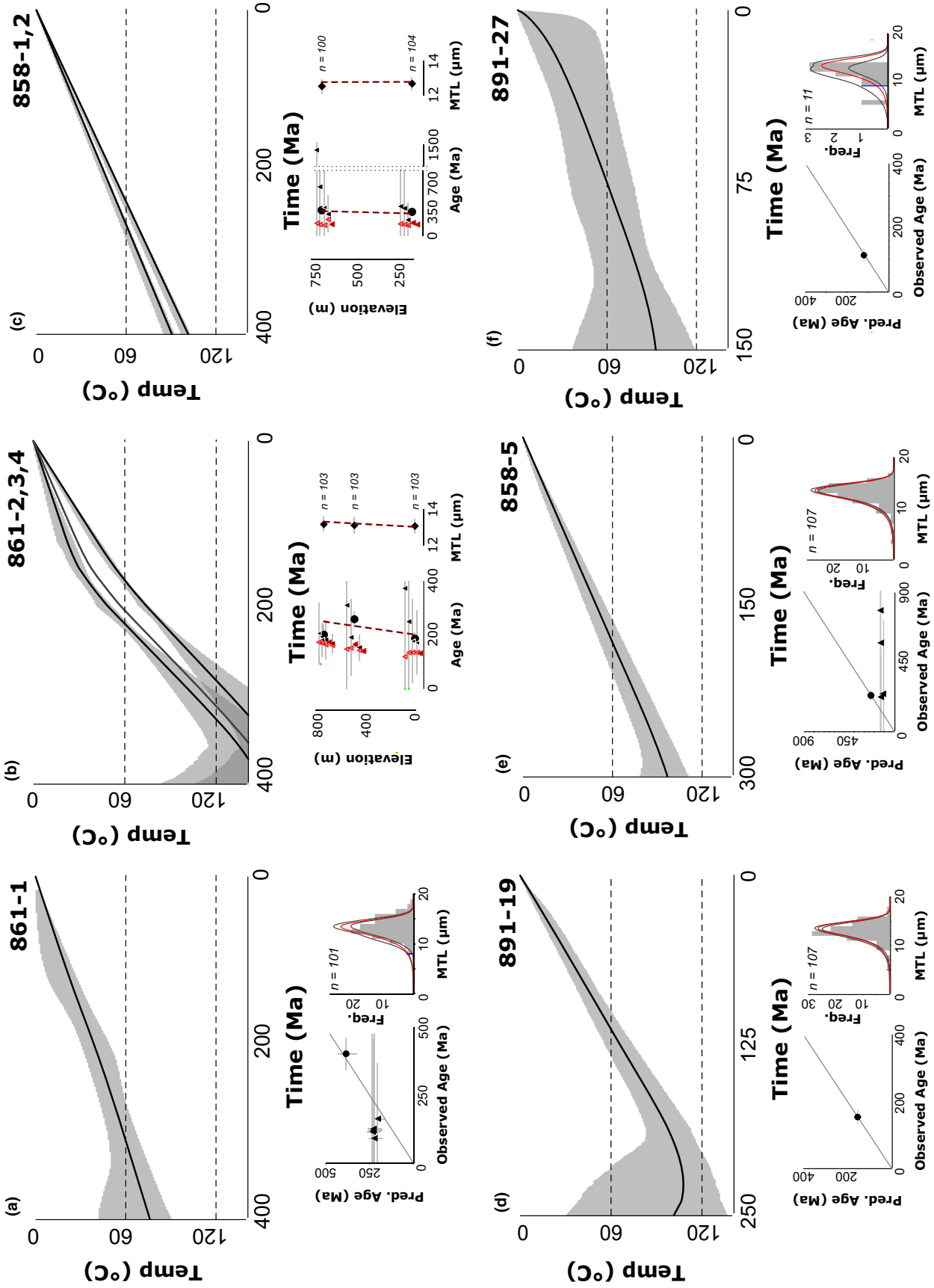
(a)
861-1
Temp (°C)
Time (Ma)
Pred. Age (Ma)
Observed Age (Ma)
Fred.
MTL (µm)
n = 101
(b)
861-2,3,4
Elevation (m)
Age (Ma)
n = 103
(c)
858-1,2
n = 100
n = 104
(d)
891-19
n = 107
(e)
858-5
(f)
891-27
n = 11

FIGURE 5 Selected thermal histories from across the Aasiaat, Sisimiut and Nuuk regions; sample locations available in Figure 1. 'Expected' thermal histories are shown as a solid black line, space between the 95% credibility intervals of the model is shaded grey and the limits of the AFT partial annealing zone (PAZ) are marked as black dashed lines. Graphs of age predictions display the comparison between predicted AFT and AHe single grain ages against their observed values (● = AFT: ▲ = AHe), while profile predictions show age, MTL and % Ro predictions as red lines or red triangles for AHe ages (spacing of AHe data is for clarity only; correct depth/elevation is that of the adjacent AFT sample). AFT track length distributions are shown as histograms with the predicted distribution highlighted as a red line. Resampling of AHe error creates large errors to accommodate all single grain ages with the combined AFT data and reveals how compatible the two age systems are. (a) 861-1: Basement sample from inland Aasiaat displaying linear protracted cooling from 400 Ma to 0 Ma (0.2°C/Myr). (b) 861-2,3,4: Basement samples from coastal Aasiaat exhibiting linear protracted cooling from the base sample (861-2) from 330 Ma to 0 Ma (0.2°C/Myr), while the top sample (861-4) exhibits protracted cooling from 370 Ma to 160 Ma (0.5°C/Myr) followed by a slower cooling rate to present (0.2°C/Myr). (c) 858-1,2: Basement samples from inland Sisimiut that display linear protracted cooling from 400 Ma to 0 Ma (0.2–0.25°C/Myr). (d) 891-19: Basement sample from coastal Sisimiut display protracted cooling from 200 Ma to 0 Ma (0.5°C/Myr). (e) 858-5: Basement sample from inland Nuuk exhibiting linear protracted cooling from 300 Ma to 0 Ma (0.3°C/Myr). (f) 891-27: Basement sample from coastal Nuuk displaying a gradually increase cooling rate from 150 Ma to 0 Ma (~0.6°C/Myr), though it must be noted the lack of track lengths has meant this thermal history is poorly constrained, observable from the large 95% confidence intervals

other data (e.g. AFT, VR, additional AHe ages). Two commonly used radiation damage models, the RDAAM model of Flowers et al. (2009) and the Gautheron et al. (2009) model, have been shown to improve modelling results (e.g. Cogné et al., 2012; Guillaume et al., 2013; Kasanzu, 2017; Leprêtre et al., 2015; Wildman et al., 2015). In this study, initial modelling trials demonstrated that the Gautheron et al. (2009) model produces AHe and AFT predictions closer to the observed values compared to RDAAM, though the differences were minor. Additionally, resampling of the error with a MCMC attempts at first to satisfy both the AFT and AHe data but, if this is not possible, expands the error bounds on AHe ages that are failing to conform to the other data, in effect removing their effect from further iterations.

The modelling approach used by Japsen et al. (2006) differs significantly to the one used here, initially comparing AFT and VR data to define a 'Default Thermal History' (an initial history-based solely on stratigraphy and assuming any sample currently resides at its maximum burial temperature) to establish the degree of fission track annealing and a maximum temperature from the VR. Once this is established, iterative forward modelling ascertains maximum palaeotemperatures and the timing of cooling, producing an AFT age and track length distribution prediction through the use of a multicompositional annealing model and the maximum likelihood method (Green, Moore, O'Brien, & Crowhurst, 2002). Each thermal history will include multiple phases of heating and cooling, whenever possible, in an attempt to improve the fission track length distribution and age predictions so to replicate the observed data as accurately as possible. All AHe ages from a single sample are then collectively tested against the best-fitting thermal history to ascertain if they are consistent with AFT and VR data; AHe samples that are consistent with the thermal history are used to improve thermal constraints, while samples that are not consistent are considered anomalous and discarded.

These two modelling approaches differ in their modelling philosophies, primary assumptions and treatment of data and justification for the use of a Bayesian approach is outlined as follows.

1 The maximum likelihood method assumes that measured data are the best representation of 'truth' and considers any subset of all data to be an accurate representation of the whole data population. In contrast, Bayes' theorem determines that data must be treated as random, assessing the results by their probability of success. This allows for objective predictions to be made based on the quality of the data and does not apply fixed model parameters, producing an assortment of models that are all probable outcomes, whereas a maximum-likelihood approach fails to account for any discrepancies within the data and can lead to unnecessary complexity.
2 The explicit parameterisation of the model to include multiple phases of heating and cooling can impose itself heavily on the final interpretation, implying additional phases of thermal change that may not actually be required or present in a sample's history. This may improve the model fit regardless of its level of complexity, whereas the Bayesian approach attempts to calculate the simplest model accounting for uncertainty in both the data and the model and will not include unnecessary periods of cooling.
3 Testing the compatibility of all AHe ages in a sample against a previously defined thermal history based on solely on AFT and VR data fails to account for the temperature constraints that individual AHe ages may provide, producing thermal histories heavily weighted by AFT data. In contrast, integrating AFT, VR and AHe together as well as data from multiple elevations provides estimates of a thermal history that satisfies all the data simultaneously, while the resampling of AHe age error identifies and effectively rejects unsuitable

individual ages while keeping those that are consistent with all other data.

These fundamental differences suggest that the use of a Bayesian approach can encapsulate more of the available data, provide models appropriate to the data quality and deliver a more objective interpretation better suited for a study of this type.

4 | THERMAL MODELLING RESULTS

All thermal histories can be found within the Data S1, while Figure 5 displays example thermal histories from the Aasiaat, Sisimiut and Nuuk regions and Figure 6 displays thermal histories from the Nuussuaq region (cf. Figure 1). Results of modelling are described below focusing on the rate and timing of cooling and, for samples that exhibit linear protracted cooling, their exit from the fission track partial annealing zone (PAZ; 120–60°C).

4.1 | Aasiaat, Sisimiut and Nuuk Regions

The three regions underlain by basement all display protracted cooling throughout the Mesozoic and Cenozoic. Within the Aasiaat region, thermal models from the northern coastline and inland display linear protracted cooling, exiting the PAZ between 300 and 250 Ma (~0.2°C/Myr; e.g. 861–1; Figure 5a), while samples located along the central coastline display protracted cooling, exiting the PAZ ~150 Ma (~0.4°C/Myr; 861–2,3,4; Figure 5b). Within the Sisimiut region inland samples exhibit protracted cooling histories exiting the PAZ between 250 and 400 Ma (0.24–0.12°C/Myr; e.g. 858–1,2; Figure 5c), while coastal samples display protracted cooling histories exiting the PAZ between ~230 Ma and ~120 Ma (0.2–0.5°C/Myr; e.g. 891–19; Figure 5d). Within the Nuuk region modelling results of inland samples display protracted cooling histories exiting the PAZ at ~175 Ma (0.3°C/Myr; 858–5; Figure 5e), whereas coastal samples all show protracted cooling from ~150 Ma exiting the PAZ ~75 Ma (0.6°C/Myr), though these histories exhibit large confidence intervals due to limited track length numbers (861–27; Figure 5f).

4.2 | Nuussuaq Region

Basement samples in the east of the Nuussuaq region display linear protracted cooling, exiting the PAZ 200–250 Ma south of the Nuussuaq Peninsula (~0.25°C/Myr; Figure 6a) and ~175 Ma to the north of Nuussuaq Peninsula (~0.3°C/Myr; Figure 6b). Samples from exposed basement on Disko Island display protracted cooling, exiting the PAZ ~400 Ma in the south (~0.17°C/Myr), while in the north the rate of cooling is slow until 90 Ma (0.1°C/Myr) before it increases to the present (0.55°C/Myr; 861–12; Figure 6c).

Sedimentary samples from the Nuussuaq region are divided into two groups: those that have experienced sufficient reheating to anneal predepositional fission tracks and those that have not. Samples from the southern extent of the basin and two samples from within the Itilli Fault Zone (GC891-7,8; Figure 6d) present no valid postdepositional thermal history as predicted. Sedimentary samples that define a postdepositional thermal history are found west of the Ikorfat Fault, on the Nuussuaq Peninsula and on the Svartenhuk Peninsula to the north (Figure 1). On the western Nuussuaq Peninsula, samples adjacent to major fault zones display heating to maximum temperature (~100°C) at ~70 Ma (~4.5°C/Myr) and linear cooling to present thereafter (~1.5°C/Myr; 861–13 & 891–6; Figure 6e,f), while two of the wells located between fault zones (Gant-1 and Gane-1) each exhibit reheating to a maximum temperature (~105°C) between ~45 and 40 Ma (4–5.5°C/Myr) and either linear cooling to present (2°C/Myr; Gant-1; Figure 6g) or protracted cooling until 10 Ma (0.9°C/Ma) followed by pronounced cooling to present (5.5°C/Myr; Gane-1; Figure 6h). On the Svartenhuk Peninsula, Umiivik-1 displays reheating to ~100°C at ~70 Ma (5.25°C/Myr), protracted cooling from ~70 Ma to ~20 Ma (0.7°C/Myr) and a period of pronounced cooling from ~20 Ma to present (2.6°C/Myr; Umiivik-1; Figure 6i). The Gro-3 well exhibits rapid cooling between 57 and 45 Ma (8.4°C/Myr; Gro-3; Figure 6j), interpreted as a modelling artefact due to narrow track length distributions, suggesting the data derived from the well are insufficient to produce a useable thermal history.

Measured AFT age and track distributions from the West Greenland Margin are predicted within error for all thermal histories, with the exception of the underannealed samples in the southern Nuussuaq Basin. VR %Ro predictions from two of the wells located on the western Nuussuaq Peninsula fit within the available range of values for each sample (Gane-1 & Gant-1), while data within Ummiivik-1 and Gro-3 cannot be reproduced due to the effect of localised igneous intrusions and inadequate AFT data. AHe data compatibility varies widely as no thermal model predicts all single grain ages within error, though ages younger than their AFT counterparts are generally well predicted and contribute to thermal histories, while ages older than the AFT age are poorly predicted and have no significant effect on the final thermal history. The inclusion of younger ages suggests the resampling of error has allowed single grain ages compatible with the counterpart AFT and VR data to be utilised within thermal modelling, providing additional thermal constraints where applicable and

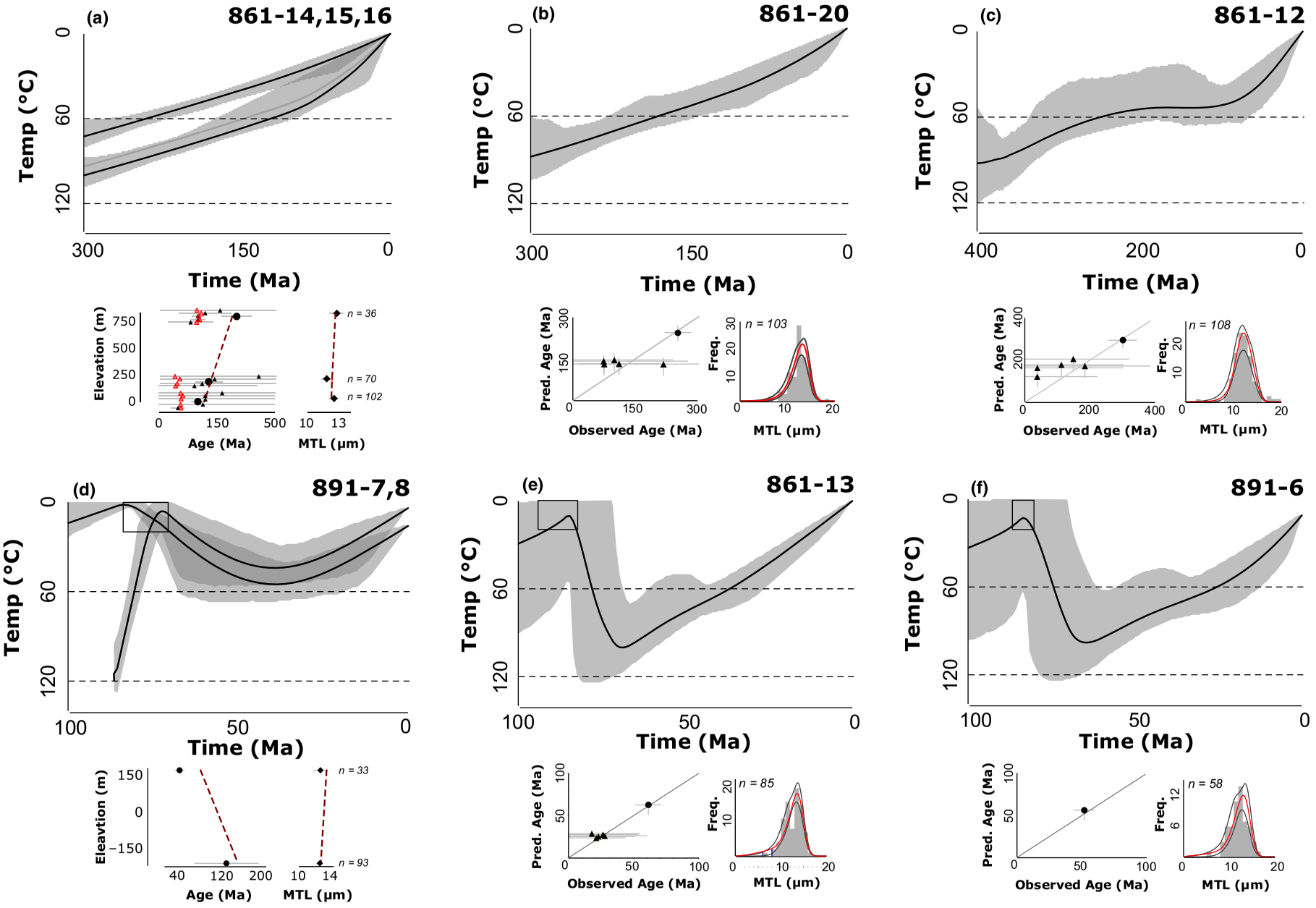
(a)
861-14,15,16
Temp (°C)
0
60
120
300
150
0
Time (Ma)
Elevation (m)
750
500
250
0
0
150
500
Age (Ma)
n = 36
n = 70
n = 102
10
13
MTL (µm)
(b)
861-20
Temp (°C)
Time (Ma)
Pred. Age (Ma)
Observed Age (Ma)
Freq.
n = 103
MTL (µm)
(c)
861-12
Temp (°C)
Time (Ma)
Pred. Age (Ma)
Observed Age (Ma)
Freq.
n = 108
MTL (µm)
(d)
891-7,8
Temp (°C)
Time (Ma)
Eleavtion (m)
150
0
−150
40
120
200
Age (Ma)
n = 33
n = 93
10
14
MTL (µm)
(e)
861-13
Temp (°C)
Time (Ma)
Pred. Age (Ma)
Observed Age (Ma)
Freq.
n = 85
MTL (µm)
(f)
891-6
Temp (°C)
Time (Ma)
Pred. Age (Ma)
Observed Age (Ma)
Freq.
n = 58
MTL (µm)

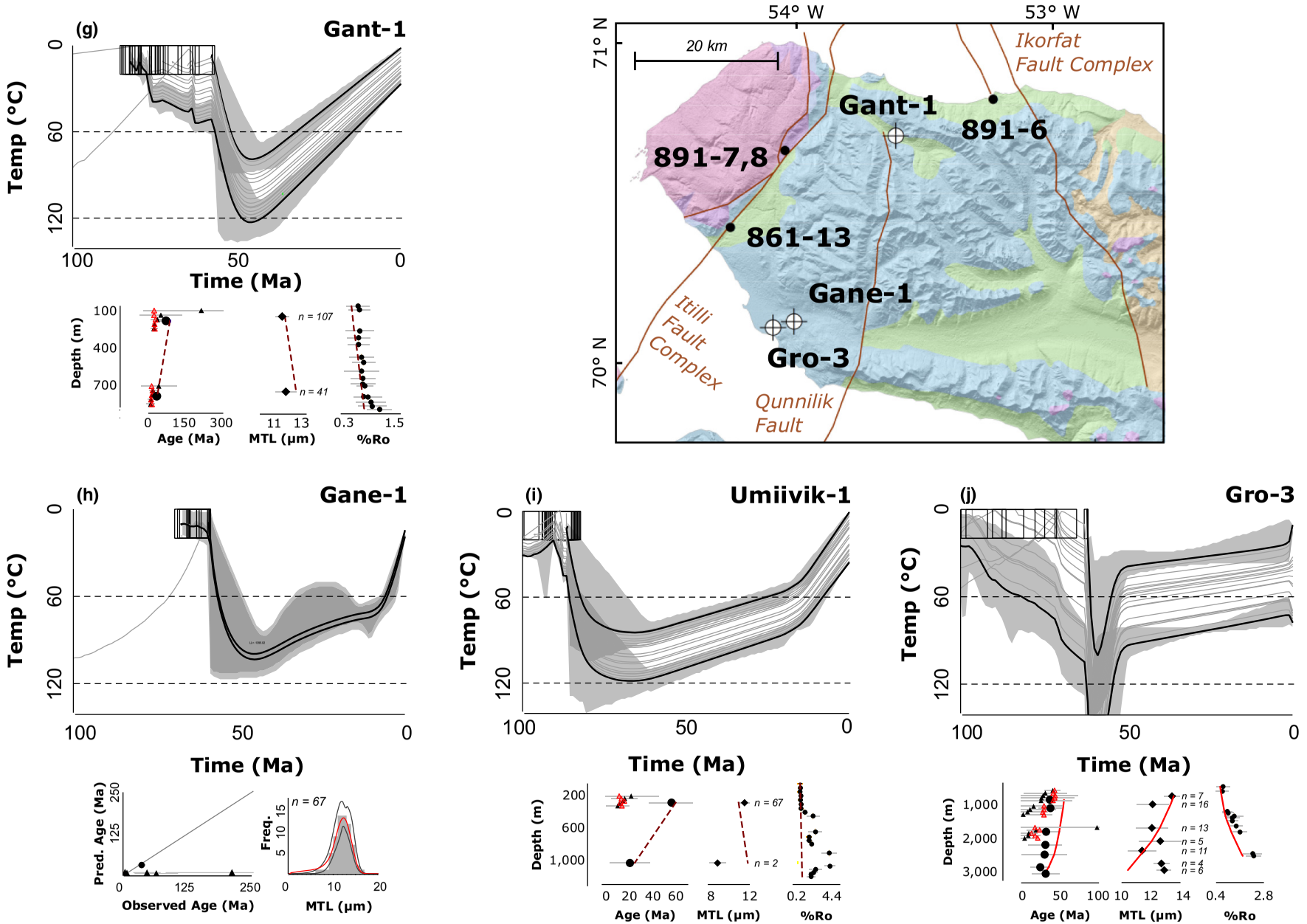

FIGURE 6 Continued

FIGURE 6 Thermal histories from across the Nuussuaq Region (see Figure 5 for explanation of thermal history layout). (a) 861-20: Basement sample taken from an exposure north of the Nuussuaq Peninsula displaying cooling linear protracted cooling from 300 Ma to 0 Ma exiting the PAZ at 180 Ma (0.3°C/Myr). (b) 861-14,15,16: Multiple basement samples from an elevation profile south of the Nuussuaq Peninsula. The highest sample (861-14) exhibits linear protracted cooling from 300 Ma to 0 Ma exiting the PAZ at 240 Ma (0.25°C/Myr), while the lower two samples (861-15,16) both exhibit protracted cooling from 300 Ma to 80 Ma (0.25°C/Myr), followed by an increase in the rate of cooling to present (0.7°C/Myr). (c) 861-12: Basement sample taken from an exposure on Disko Island displaying cooling protracted cooling form 400 Ma to 200 Ma (0.2°C/Myr) and accelerated cooling from 100 Ma to 0 Ma (0.6°C/Myr). (d) 891-7,8 (strat age: 83–70.6 Ma): Sedimentary samples taken from the fault foot wall of the Itilli Fault Complex displaying heating from 83 Ma to 40 Ma (5.25°C/Myr) and cooling to present (1°C/Myr). As the history does not enter the PAZ, we can conclude these samples do not provide a robust postdepositional thermal history due to a lack of heating/burial, likely due to uplift of the Itilli Fault Zone in the Late Cretaceous. (e) 891-6 (strat age: 83–70.6 Ma): Sedimentary samples taken from the Ikorfat Fault Zone displaying heating from 85 Ma to 65 Ma (4.5°C/Myr) and cooling to present (1.6°C/Myr) implying burial through the Late Cretaceous and uplift of the Ikorfat Fault Zone in the Late Maastrichtian. (f) 861-13 (stratigraphic age: 95–70.6 Ma): Sedimentary samples taken from the fault foot wall of the Itilli Fault Complex displaying heating from 85 Ma to 70 Ma (4.5°C/Myr) and cooling to present (1.4°C/Myr) implying burial through the Late Cretaceous and uplift of the Itilli Fault footwall in the Late Maastrichtian. (g) Gane-1 (65–62 Ma): Sedimentary sample taken from the half graben between the Qunnilik Fault and Itilli Fault Complex exhibiting heating from 60 Ma to 45 Ma (5.7°C/Myr), protracted cooling to 10 Ma (0.9°C/Myr) and accelerated cooling to present (5.6°C/Myr). This history implies burial under the volcanic stratigraphy through the Palaeogene followed by widespread erosion, augmented by glaciation in the Neogene. (h) Gant-1 (86–57 Ma): Sedimentary samples taken from the half graben between the Ikorfat Fault Zone and the edge of the Qunnilik Fault display heating from 58 Ma to 40 Ma (3.9°C/Myr) and protracted cooling to present (1.9°C/Myr). This thermal history implies burial under the volcanic stratigraphy through the Palaeogene followed by widespread erosion of the overburden to present. (i) Ummiivik-1 (strat age: 112–87 Ma): Sedimentary samples taken from the Svartenhuk Peninsula displaying heating between 90 and 70 Ma (5.25°C/Myr) and steady protracted cooling from here to ~20 Ma (0.7°C/Myr). Accelerated cooling is observed from ~20 Ma to 0 Ma (2.6°C/Myr) likely as the result of atmospheric cooling and glaciation in the region. (j) Gro-3 (strat age: 112–62 Ma): Sedimentary samples taken from the half graben between Qunnilik Fault and Itilli Fault Complex displaying heating between 63 Ma and 57.5 Ma (24°C/Myr), rapid cooling to 45 Ma (8.4°C/Myr) steady protracted cooling from here to present (0.4°C/Myr). This thermal history differs greatly to those of Gane-1 and Gant-1 suggesting that this thermal history cannot be considered representative of the Gro-3 thermal history and is likely an artefact of the lack of track lengths. The map of the western Nuussuaq Peninsula outlines the location of 861–13, 891–7,8, 891–6, Gane-1, Gant-1 and Gro-3, demonstrating the relationship between the samples adjacent to fault zones and those in half graben between them

effectively removing incompatible older ages. Moreover, the lack of models with all ages included demonstrates that dispersion across the samples cannot be exclusively explained by the radiation damage model alone and may be the result of factors, as of yet, unaccounted for in the modelling approach (e.g. implantation, zonation or microinclusions). Although AHe data predictions vary, these integrated Bayesian thermal histories are valuable interpretative tools, highlighting an effective approach to deal with complex data sets and help infer a geological history for much of the West Greenland Margin.

5 | DISCUSSION

5.1 | Geological history of the West Greenland margin

Results from the southern extent of the margin studied here indicate that a protracted erosional regime has been in place since the end of rifting, showing no indication of an erosional response to Cenozoic tectonic rejuvenation. The protracted nature of cooling suggests that little change has occurred within the erosion regime through the Mesozoic and Cenozoic and implies that uplift of the margin during rifting is the most likely source of the elevated topography. The modern geomorphology of the margin may likely be the result of the underlying Archaean/Proterozoic geology and glaciation in the region, the latter causing erosion at different rates dependent on elevation, effectively preserving much of the higher topography while differentially eroding the margin (Strunk et al., 2017; Figure 7). This interpretation is consistent with that of several continental margins in the North Atlantic realm (Hendriks & Andriessen, 2002; Johnson & Gallagher, 2000; McGregor, Nielsen, & Stephenson, 2014; McGregor, Nielsen, Stephenson, Petersen, & Macdonald, 2013; Nielsen et al., 2009; Pedersen, Nielsen, & Gallagher, 2012) and implies that the elevated topography of the southern margin is Mesozoic in age and not the result of Late Cenozoic tectonic uplift.

Thermal histories from the western the Nuussuaq Peninsula outline extension and uplift in the Late Cretaceous/Early Palaeocene and its effect on the later clastic and volcanic stratigraphy. Samples adjacent to major basinal fault zones display the onset of cooling ~70 Ma (861–13, 891–6; Figure 6e,f), likely as the result of footwall uplift during extensional tectonism in the Late Cretaceous, while samples located between the two major fault zones display reheating during and after this time (Gane-1, Gant-1; Figure 6g,h), likely as a result of subsidence and the deposition of the Kangilia, Agatdal and Quikavsak formations in half graben structures. Furthermore, the folding of the Itilli Formation perpendicular to the Itilli Fault zone and the

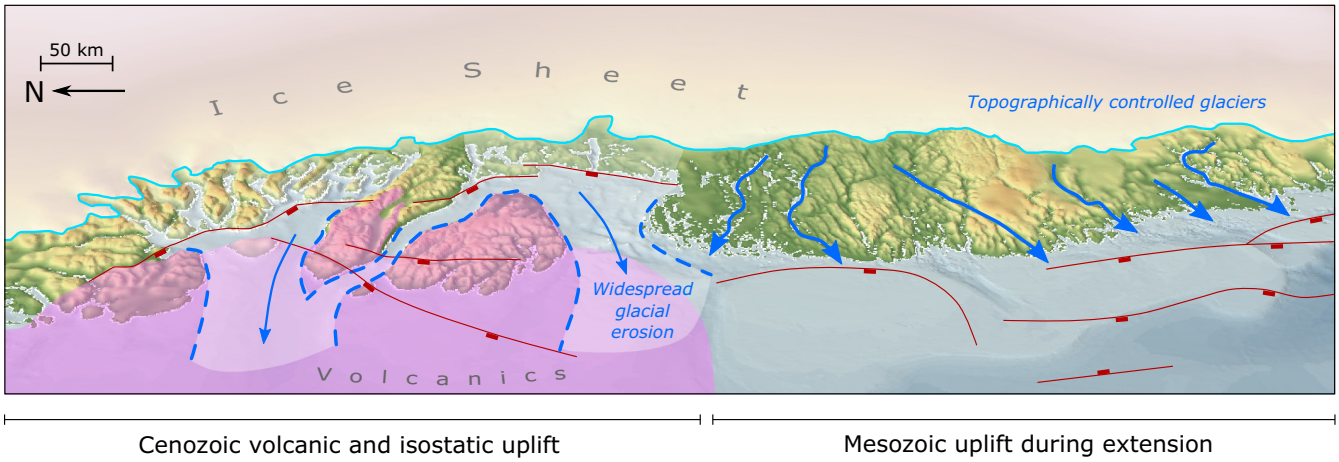

FIGURE 7 Overview of the study area outlining the key differences between the Nuussuaq Region and the rest of the SW margin. The underling geology of each area varies dramatically, from Archaean/Proterozoic basement in the SW to Cretaceous/Palaeocene sediments and Palaeocene/Eocene volcanics in the north, corresponding to the change in landscape. The extensional history of the SW margin yields many rift-related faults and subsidence offshore, while in the Nuussuaq Region, faulting and subsidence appear further onshore suggesting a contrast in structural domains. Moreover, the glacial history of both sections of the margin differ heavily, with the Nuussuaq Region experiencing significant widespread glacial erosion, while in the south much of the erosion is constrained by the topography. These variations in geology, structure and glacial history demonstrate the dichotomy between the Nuussuaq Region and the SW margin, suggesting the topography of both are likely sourced from separate sources, Mesozoic rifting in the south and Cenozoic volcanism and isostasy in the north

lack of thermal annealing in samples atop the Itilli Fault Zone (GC891-7,8; Figure 6d), implies uplift in the Palaeocene lead to folding of strata SE of the fault zone and restricted the burial and reheating of these samples. This selection of thermal histories demonstrates how the basin tectonically evolved during the Late Cretaceous/Early Palaeocene, in accordance with the documented stratigraphy.

Pronounced Late Cenozoic cooling within the Gane-1 and Umiivik-1 thermal histories (Figure 6h,i) is interpreted as a response to climatic changes across the North Atlantic. Cooling exhibited in these thermal histories postdates a decline in surface temperatures observed at the Eocene-Oligocene boundary (Bernard et al., 2016; Eldrett, Greenwood, Harding, & Huber, 2009) and is coeval with evidence of early glaciation across Greenland (Thiede et al., 2011), suggesting glaciation has been present across the margin since the Neogene. The coupling of a decrease in surface temperatures and a more intensive erosional regime during the Neogene and Quaternary is likely to have produced a significant period of cooling similar to that observed in the two wells.

The newly produced thermal histories presented here do not indicate the occurrence of episodic Late Cenozoic uplift and erosion within the Nuussuaq Basin, yet the height of the modern topography and the presence of Mid-Palaeocene marine stratigraphy at ~1200 m elevation (Piasecki et al., 1992) does imply uplift of a significant amplitude has occurred following the Palaeocene. Differential glacial erosion across West Greenland (Medvedev, Souche, & Hartz, 2013), East Greenland (Medvedev, Hartz, & Podladchikov, 2008) and Scandinavia (Medvedev & Hartz, 2015) has been shown to produce significant topographical uplift (~800 m) as a flexural isostatic response to the unloading of the lithosphere. The onset of cooling in all sedimentary samples from the Nuussuaq Basin occurs prior to ~40 Ma, suggesting the end of volcanism in the Mid-Eocene was followed by widespread erosion of the newly formed volcanic pile (Figure 3) supporting this interpretation. Although the extent of erosion-related uplift is significant, it may not account for all the total uplift within the Nuussuaq Basin suggesting additional mechanisms are required to elevate the topography. Numerical modelling and geological observations from several large igneous provinces (LIPs) demonstrate that doming of the lithosphere can occur before and during volcanism (Campbell, 2007; Peate & Bryan, 2008) and could lift the underlying topography up relative to sea level while burying samples under an expanding lava pile, producing similar thermal histories to those presented here. This combination of volcanism in the Palaeogene and continuous erosion from the Mid-Eocene to present are likely to have significantly affected the landscape of the Nuussuaq region and created the modern-elevated topography without the need for episodic Late Cenozoic tectonism (Figure 7).

5.2 | Implications for Late Cenozoic uplift in the North Atlantic

Late Cenozoic episodic uplift is a proposed source of the elevated continental margins across the Northern Atlantic and remains a contentious issue within the literature (e.g.

Anell, Thybo, & Artemieva, 2009; Cloetingh, Gradstein, Kooi, Grant, & Kaminski, 1990; Eyles, 1996; Gołędowski, Nielsen, & Clausen, 2012; Green, Lidmar-Bergström, Japsen, Bonow, & Chalmers, 2013; Japsen & Chalmers, 2000; Japsen et al., 2010; McGregor et al., 2013; Nielsen et al., 2009). The results of this study suggest postrift uplift along the West Greenland Margin is only recorded within the Nuussuaq Basin during the Cenozoic and no evidence of any significant uplift is documented along the southern extent of the margin. The contrast of these new inferences with previously cited evidence of uplift in the Neogene and the implications of the present results are briefly discussed below.

The interpretation of low-relief high-elevation surfaces as peneplains (uplifted flood plains) and offshore tilted unconformities as the result of uplift onshore has been previously presented as evidence for tectonic rejuvenation and uplift along the Scandinavian, Greenland, Canadian and British continental margins (e.g. Bonow, Japsen, & Nielsen, 2014; Chalmers, 2000; Green, Japsen, Chalmers, Bonow, & Duddy, 2018; Lidmar-Bergström, Ollier, & Sulebak, 2000; Riis, 1996; Rowberry, 2008); however, several recent studies have suggested other processes are the source of these features. Recent cosmogenic isotope studies from across West Greenland suggested the modern geomorphology is likely the result of glaciation, where warm-based glaciers focus erosion along preglacial river valleys, forming deeply incised fjords and cold-based glaciers limit erosion in highland areas, resulting in elevated low-relief surfaces (Egholm et al., 2017; Strunk et al., 2017). These conclusions would imply the modern landscape of the SW margin is simply the result of glacial erosion of an elevated rift flank, balanced by the redistribution of sediments offshore. Moreover, tilted offshore unconformities are most likely the result of flexural tilting of the lithosphere basinwards due to loading and thermal subsidence following the end of rifting (Geoffroy et al., 2001) and do not require Cenozoic onshore tectonism. The source of the unconformities themselves is enigmatic but has been linked to regional uplift (Chalmers, 2000), simple nondepositional hiatuses (McGregor et al., 2013) and glaciation (Chalmers, 2000). These interpretations of the onshore geomorphology and offshore geometries support the model presented here of how central West Greenland and the Nuussuaq Basin have evolved, suggesting that Late Cenozoic tectonism and uplift is not required to elevate the coastal topography.

6 | SUMMARY AND CONCLUSIONS

In this study, AFT, AHe and VR data are combined and modelled jointly to resolve the thermal history of Central West Greenland and the Nuussuaq Basin. The modelling methodology enabled objective thermal histories to be derived from this complex data set that are consistent with the existing AFT, VR and AHe data and stratigraphic constraints collectively yielding an appropriate regional interpretation.

Proterozoic samples along the south of the margin provide thermal histories showing protracted cooling throughout the Mesozoic and Cenozoic, while sedimentary samples from within the Nuussuaq Basin outline uplift and subsidence associated with rifting in the Late Cretaceous and widespread volcanism in the Palaeogene. Thermal histories from the western Nuussuaq Peninsula suggest significant uplift in the Late Cretaceous and Palaeocene, accommodated by displacement on fault zones, formed half grabens that were later filled by the overlying sediments and volcanics, inferred from the timing of cooling in samples adjacent to major fault zones and the documented stratigraphy. The end of volcanism in the Eocene sees the entire region begin a prolonged period of erosion and intense glacial denudation likely generating significant flexural feedback from the lithosphere. The combination of uplift during volcanism and the isostatic response to unroofing are the likely sources of the Nuussuaq Basin's modern-elevated topography and suggests Late Cenozoic tectonism is not necessary.

ACKNOWLEDGEMENTS

Tim Redfield and a second anonymous reviewer are thanked for their constructive comments. The work contained in this publication contains work conducted during a PhD study undertaken as part of the Natural Environment Research Council (NERC) Centre for Doctoral Training (CDT) in Oil & Gas [grant number NEM00578X/1] and is sponsored by the University of Aberdeen.

REFERENCES

Abdelmalak, M. M., Geoffroy, L., Angelier, J., Bonin, B., Callot, J. P., Gélard, J. P., & Aubourg, C. (2012). Stress fields acting during lithosphere breakup above a melting mantle: A case example in West Greenland. *Tectonophysics*, *581*, 132–143. https://doi.org/10.1016/j.tecto.2011.11.020

Alsulami, S., Paton, D. A., & Cornwell, D. G. (2015). Tectonic variation and structural evolution of the West Greenland continental margin. *AAPG Bulletin*, *99*(9), 1689–1711. https://doi.org/10.1306/03021514023

Anell, I., Thybo, H., & Artemieva, I. (2009). Cenozoic uplift and subsidence in the North Atlantic region: Geological evidence revisited. *Tectonophysics*, *474*(1), 78–105. https://doi.org/10.1016/j.tecto.2009.04.006

Bernard, T., Steer, P., Gallagher, K., Szulc, A., Whitham, A., & Johnson, C. (2016). Evidence for Eocene-Oligocene glaciation in the landscape of the East Greenland margin. *Geology*, *44*(11), 895–898. https://doi.org/10.1130/G38248.1

Bonow, J. M., Japsen, P., & Nielsen, T. F. D. (2014). High-level landscapes along the margin of southern East Greenland—A record of tectonic uplift and incision after breakup in the NE Atlantic.

Brown, R. W., Beucher, R., Roper, S., Persano, C., Stuart, F., & Fitzgerald, P. (2013). Natural age dispersion arising from the analysis of broken crystals. Part I: Theoretical basis and implications for the apatite (U–Th)/He thermochronometer. *Geochimica et Cosmochimica Acta*, *122*, 478–497. https://doi.org/10.1016/j.gca.2013.05.041

Brown, R., & Green, P. (1991). Discussion on thermal and tectonic history of the East Midlands shelf (onshore UK) and surrounding regions assessed by apatite fission track analysis, J. Geol. Soc. London, Vol. 146, 1989, pp. 755-773. *Journal of the Geological Society*, *148*, 785–787.

Campbell, I. H. (2007). Testing the plume theory. *Chemical Geology*, *241*(3), 153–176. https://doi.org/10.1016/j.chemgeo.2007.01.024

Chalmers, J. A. (2000). Offshore evidence for Neogene uplift in central West Greenland. *Global and Planetary Change*, *24*(3), 311–318. https://doi.org/10.1016/S0921-8181(00)00015-1

Chalmers, J. A., Green, P., Japsen, P., & Rasmussen, E. S. (2010). The Scandinavian mountains have not persisted since the Caledonian orogeny. A comment on Nielsen et al. (2009a). *Journal of Geodynamics*, *50*(2), 94–101.https://doi.org/10.1016/j.jog.2010.02.001

Chalmers, J., Pulvertaft, T., Marcussen, C., & Pedersen, A. (1999). New insight into the structure of the Nuussuaq Basin, central West Greenland. *Marine and Petroleum Geology*, *16*(3), 197–224. https://doi.org/10.1016/S0264-8172(98)00077-4

Cloetingh, S., Gradstein, F., Kooi, H., Grant, A., & Kaminski, M. (1990). Plate reorganization: a cause of rapid late Neogene subsidence and sedimentation around the North Atlantic? *Journal of the Geological Society*, *147*(3), 495–506. https://doi.org/10.1144/gsjgs.147.3.0495

Cogné, N., Gallagher, K., Cobbold, P. R., Riccomini, C., & Gautheron, C. (2012). Post-breakup tectonics in southeast Brazil from thermochronological data and combined inverse-forward thermal history modelling. *Journal of Geophysical Research*, *117*, B11413, https://doi.org/10.1029/2012JB009340

Dalhoff, F., Chalmers, J. A., Gregersen, U., Nøhr-Hansen, H., Rasmussen, J. A., & Sheldon, E. (2003). Mapping and facies analysis of Paleocene–Mid-Eocene seismic sequences, offshore southern West Greenland. *Marine and Petroleum Geology*, *20*(9), 935–986. https://doi.org/10.1016/j.marpetgeo.2003.09.004

Dam, G., & Nøhr-Hansen, H. (2001). Mantle plumes and sequence stratigraphy; late Maastrichtian–early Paleocene of West Greenland. *Bulletin of the Geological Society of Denmark*, *48*, 189–207.

Dam, G., Pedersen, G. K., Sønderholm, M., Midtgaard, H. H., Larsen, L. M., Nøhr-Hansen, H., & Pedersen, A. K. (2009). Lithostratigraphy of the Cretaceous-Paleocene Nuussuaq Group, Nuussuaq Basin, West Greenland. *Geological Survey of Denmark and Greenland Bulletin*, *19*, 171.

Djimbi, D. M., Gautheron, C., Roques, J., Tassan-Got, L., Gerin, C., & Simoni, E. (2015). Impact of apatite chemical composition on (U-Th)/He thermochronometry: An atomistic point of view. *Geochimica et Cosmochimica Acta*, *167*, 162–176. https://doi.org/10.1016/j.gca.2015.06.017

Donelick, R. A., O'Sullivan, P. B., & Ketcham, R. A. (2005). Apatite fission-track analysis. *Reviews in Mineralogy and Geochemistry*, *58*(1), 49–94. https://doi.org/10.2138/rmg.2005.58.3

Egholm, D. L., Jansen, J. D., Brædstrup, C. F., Pedersen, V. K., Andersen, J. L., Ugelvig, S. V., … Knudsen, M. F. (2017). Formation of plateau landscapes on glaciated continental margins. *Nature Geoscience*, *10*(8), 592–597. https://doi.org/10.1038/ngeo2980

Eidvin, T., Riis, F., & Rasmussen, E. S. (2014). Oligocene to Lower Pliocene deposits of the Norwegian continental shelf, Norwegian Sea, Svalbard, Denmark and their relation to the uplift of Fennoscandia: A synthesis. *Marine and Petroleum Geology*, *56*, 184–221. https://doi.org/10.1016/j.marpetgeo.2014.04.006

Eldrett, J. S., Greenwood, D. R., Harding, I. C., & Huber, M. (2009). Increased seasonality through the Eocene to Oligocene transition in northern high latitudes. *Nature*, *459*(7249), 969. https://doi.org/10.1038/nature08069

Eyles, N. (1996). Passive margin uplift around the North Atlantic region and its role in Northern Hemisphere late Cenozoic glaciation. *Geology*, *24*(2), 103–106. https://doi.org/10.1130/0091-7613(1996)024<0103:PMUATN>2.3.CO;2

Farley, K. A., Wolf, R. A., & Silver, L. T. (1996). The effects of long alpha-stopping distances on (U □ Th)/He ages. *Geochimica et cosmochimica acta*, *60*(21), 4223–4229. https://doi.org/10.1016/S0016-7037(96)00193-7

Fitzgerald, P., Baldwin, S. L., Webb, L., & O'Sullivan, P. B. (2006). Interpretation of (U–Th)/He single grain ages from slowly cooled crustal terranes: a case study from the Transantarctic Mountains of southern Victoria Land. *Chemical Geology*, *225*(1), 91–120. https://doi.org/10.1016/j.chemgeo.2005.09.001

Flowers, R. M., & Kelley, S. A. (2011). Interpreting data dispersion and "inverted" dates in apatite (U–Th)/He and fission-track datasets: an example from the US midcontinent. *Geochimica et Cosmochimica Acta*, *75*(18), 5169–5186. https://doi.org/10.1016/j.gca.2011.06.016

Flowers, R. M., Ketcham, R. A., Shuster, D. L., & Farley, K. A. (2009). Apatite (U-Th)/He thermochronometry using a radiation damage accumulation and annealing model. *Geochimica et Cosmochimica Acta*, *73*(8), 2347–2365. https://doi.org/10.1016/j.gca.2009.01.015

Gallagher, K. (2012). Transdimensional inverse thermal history modelling for quantitative thermochronology. *Journal of Geophysical Research*, *117*, B02408. https://doi.org/10.1029/2011JB008825

Gallagher, K., & Brown, R. (1997). The onshore record of passive margin evolution. *Journal of the Geological Society*, *154*(3), 451–457. https://doi.org/10.1144/gsjgs.154.3.0451

Gautheron, C., Barbarand, J., Ketcham, R. A., Tassan-Got, L., van der Beek, P., Pagel, M., … Fialin, M. (2013). Chemical influence on α-recoil damage annealing in apatite: Implications for (U–Th)/He dating. *Chemical Geology*, *351*, 257–267. https://doi.org/10.1016/j.chemgeo.2013.05.027

Gautheron, C., Tassan-Got, L., Barbarand, J., & Pagel, M. (2009). Effect of alpha-damage annealing on apatite (U-Th)/He thermochronology. *Chemical Geology*, *266*(3–4), 157–170. https://doi.org/10.1016/j.chemgeo.2009.06.001

Geoffroy, L., Callot, J., Scaillet, S., Skuce, A., Gélard, J., Ravilly, M., … Perrot, K. (2001). Southeast Baffin volcanic margin and the North American-Greenland plate separation. *Tectonics*, *20*(4), 566–584. https://doi.org/10.1029/2001TC900003

Gerin, C., Gautheron, C., Oliviero, E., Bachelet, C., Djimbi, D. M., Seydoux-Guillaume, A. M., … Garrido, F. (2017). Influence of vacancy damage on He diffusion in apatite, investigated at atomic to mineralogical scales. *Geochimica et Cosmochimica Acta*, *197*, 87–103. https://doi.org/10.1016/j.gca.2016.10.018

Gołędowski, B., Nielsen, S. B., & Clausen, O. R. (2012). Patterns of Cenozoic sediment flux from western Scandinavia. *Basin Research*, *24*(4), 377–400. https://doi.org/10.1111/j.1365-2117.2011.00530.x

Green, P. F. (1989). Thermal and tectonic history of the East Midlands shelf (onshore UK) and surrounding regions assessed by apatite fission track analysis. *Journal of the Geological Society*, *146*(5), 755–773. https://doi.org/10.1144/gsjgs.146.5.0755

Green, P. F., Japsen, P., Chalmers, J. A., Bonow, J. M., & Duddy, I. R. (2018). Post-breakup burial and exhumation of passive continental margins: Seven propositions to inform geodynamic models. *Gondwana Research*, *53*, 58–81. https://doi.org/10.1016/j.gr.2017.03.007

Green, P. F., Lidmar-Bergström, K., Japsen, P., Bonow, J. M., & Chalmers, J. A. (2013). Stratigraphic landscape analysis, thermochronology and the episodic development of elevated, passive continental margins. *Geological Survey of Denmark & Greenland Bulletin*, (30), 9–150.

Green, P. F., Moore, M. E., Gibson, H. J., & O'Brien, C. O. (2004). Thermal history of thirty-three samples from outcrops and boreholes in west Greenland, based on AFTA®. *Geotrack Report*, *891*, 1–98.

Green, P. F., Moore, M. E., O'Brien, C. O., & Crowhurst, P. V. (2002). Thermal history of four samples of basement from outcrops in west Greenland, based on AFTA® and apatite (U-TH)/He dating. *Geotrack Report*, *850*, 1–27.

Green, P. F., Moore, M. E., O'Brien, C. O., & Crowhurst, P. V. (2003a). Thermal history of six samples from outcrops in west Greenland, based on AFTA® and apatite (U-TH)/He dating. *Geotrack Report*, *858*, 1–40.

Green, P. F., Moore, M. E., O'Brien, C. O., & Crowhurst, P. V. (2003b). Thermal history of twenty samples from outcrops in west Greenland, based on AFTA® and apatite (U-TH)/He dating. *Geotrack Report*, *861*, 1–73.

Green, P. F., Moore, M. E., O'Brien, C. O., & Crowhurst, P. V. (2003c). Thermal history reconstruction in the Ataa-1, Gane-1, Gant-1, Gro-3 and Umiivik-1 boreholes, onshore West Greenland, based on AFTA1, Vitrinite Reflectance and Apatite (U–Th)/He dating. *Geotrack Report*, *883*, 1–136.

Gregersen, U., Hopper, J. R., & Knutz, P. C. (2013). Basin seismic stratigraphy and aspects of prospectivity in the NE Baffin Bay, Northwest Greenland. *Marine and Petroleum Geology*, *46*, 1–18. https://doi.org/10.1016/j.marpetgeo.2013.05.013

Guillaume, B., Gautheron, C., Simon-Labric, T., Martinod, J., Roddaz, M., & Douville, E. (2013). Dynamic topography control on Patagonian relief evolution as inferred from low temperature thermochronology. *Earth and Planetary Science Letters*, *364*, 157–167. https://doi.org/10.1016/j.epsl.2012.12.036

Hansen, K. (1996). Thermotectonic evolution of a rifted continental margin: fission track evidence from the Kangerlussuaq area, SE Greenland. *Terra Nova*, *8*(5), 458–469. https://doi.org/10.1111/j.1365-3121.1996.tb00771.x

Hendriks, B. W., & Andriessen, P. A. (2002). Pattern and timing of the post-Caledonian denudation of northern Scandinavia constrained by apatite fission-track thermochronology. *Geological Society, London, Special Publications*, *196*(1), 117–137. https://doi.org/10.1144/GSL.SP.2002.196.01.08

Hendriks, B. W. H., & Redfield, T. F. (2005). Apatite fission track and (U-Th)/He data from Fennoscandia: An example of underestimation of fission track annealing in apatite. *Earth and Planetary Science Letters*, *236*(1–2), 443–458. https://doi.org/10.1016/j.epsl.2005.05.027

Japsen, P., Bonow, J. M., Green, P. F., Chalmers, J. A., & Lidmar-Bergström, K. (2006). Elevated, passive continental margins: Long-term highs or Neogene uplifts? New evidence from West Greenland. *Earth and Planetary Science Letters*, *248*(1), 330–339. https://doi.org/10.1016/j.epsl.2006.05.036

Japsen, P., & Chalmers, J. A. (2000). Neogene uplift and tectonics around the North Atlantic: overview. *Global and Planetary Change*, *24*(3–4), 165–173. https://doi.org/10.1016/S0921-8181(00)00006-0

Japsen, P., Green, P., Bonow, J., Rasmussen, E., Chalmers, J., & Kjennerud, T. (2010). Episodic uplift and exhumation along North Atlantic passive margins: implications for hydrocarbon prospectivity, Geological Society, London, Petroleum Geology Conference series 2010. Geological Society of London, pp. 979-1004.

Japsen, P., Green, P. F., & Chalmers, J. A. (2005). Separation of Palaeogene and Neogene uplift on Nuussuaq, West Greenland. *Journal of the Geological Society*, *162*(2), 299–314. https://doi.org/10.1144/0016-764904-038

Johannessen, K. C., Kohlmann, F., Ksienzyk, A. K., Dunkl, I., & Jacobs, J. (2013). Tectonic evolution of the SW Norwegian passive margin based on low-temperature thermochronology from the innermost Hardangerfjord area. *Norwegian Journal of Geology/Norsk Geologisk Forening*, *93*, 243–260.

Johnson, C., & Gallagher, K. (2000). A preliminary Mesozoic and Cenozoic denudation history of the North East Greenland onshore margin. *Global and Planetary Change*, *24*(3), 261–274. https://doi.org/10.1016/S0921-8181(00)00012-6

Kasanzu, C. H. (2017). Apatite fission track and (U-Th)/He thermochronology from the Archean Tanzania Craton: Contributions to cooling histories of Tanzanian basement rocks. *Geoscience Frontiers*, *8*(5), 999–1007. https://doi.org/10.1016/j.gsf.2016.09.007

Kohn, B. P., Lorencak, M., Gleadow, A. J., Kohlmann, F., Raza, A., Osadetz, K. G., & Sorjonen-Ward, P. (2009). A reappraisal of low-temperature thermochronology of the eastern Fennoscandia Shield and radiation-enhanced apatite fission-track annealing. *Geological Society, London, Special Publications*, *324*(1), 193–216. https://doi.org/10.1144/SP324.15

Larsen, L. M., Pedersen, A. K., Tegner, C., Duncan, R. A., Hald, N., & Larsen, J. G. (2016). Age of Tertiary volcanic rocks on the West Greenland continental margin: volcanic evolution and event correlation to other parts of the North Atlantic Igneous Province. *Geological Magazine*, *153*(3), 487–511. https://doi.org/10.1017/S0016756815000515

Larson, S. Å., Cederbom, C. E., Tullborg, E. L., & Stiberg, J. P. (2006). Comment on "Apatite fission track and (U–Th)/He data from Fennoscandia: An example of underestimation of fission track annealing in apatite" by Hendriks and Redfield [Earth Planet. Sci. Lett. 236 (443–458)]. *Earth and Planetary Science Letters*, *248*(1–2), 561–568. https://doi.org/10.1016/j.epsl.2006.06.018

Leprêtre, R., Missenard, Y., Barbarand, J., Gautheron, C., Saddiqi, O., & Pinna-Jamme, R. (2015). Postrift history of the eastern central Atlantic passive margin: Insights from the Saharan region of South Morocco. *Journal of Geophysical Research: Solid Earth*, *120*(6), 4645–4666.

Lidmar-Bergström, K., Ollier, C., & Sulebak, J. (2000). Landforms and uplift history of southern Norway. *Global and Planetary Change*, *24*(3), 211–231. https://doi.org/10.1016/S0921-8181(00)00009-6

McGregor, E. D., Nielsen, S. B., & Stephenson, R. A. (2014). Basin evolution in the Davis Strait area (West Greenland and conjugate East Baffin/Labrador passive margins) from thermostratigraphic and

subsidence modelling of well data: Implications for tectonic evolution and petroleum systems. *Bulletin of Canadian Petroleum Geology*, *62*(4), 311–329. https://doi.org/10.2113/gscpgbull.62.4.311

McGregor, E., Nielsen, S., Stephenson, R., Petersen, K., & Macdonald, D. (2013). Long-term exhumation of a Palaeoproterozoic orogen and the role of pre-existing heterogeneous thermal crustal properties: a fission-track study of SE Baffin Island. *Journal of the Geological Society*, *170*(6), 877–891. https://doi.org/10.1144/jgs2012-146

Medvedev, S., & Hartz, E. H. (2015). Evolution of topography of post-Devonian Scandinavia: Effects and rates of erosion. *Geomorphology*, *231*, 229–245. https://doi.org/10.1016/j.geomorph.2014.12.010

Medvedev, S., Hartz, E. H., & Podladchikov, Y. Y. (2008). Vertical motions of the fjord regions of central East Greenland: impact of glacial erosion, deposition, and isostasy. *Geology*, *36*(7), 539–542. https://doi.org/10.1130/G24638A.1

Medvedev, S., Souche, A., & Hartz, E. H. (2013). Influence of ice sheet and glacial erosion on passive margins of Greenland. *Geomorphology*, *193*, 36–46. https://doi.org/10.1016/j.geomorph.2013.03.029

Nielsen, S. B., Gallagher, K., Leighton, C., Balling, N., Svenningsen, L., Jacobsen, B. H., … Egholm, D. L. (2009). The evolution of western Scandinavian topography: a review of Neogene uplift versus the ICE (isostasy–climate–erosion) hypothesis. *Journal of Geodynamics*, *47*(2), 72–95. https://doi.org/10.1016/j.jog.2008.09.001

Oakey, G. N., & Chalmers, J. A. (2012). A new model for the Paleogene motion of Greenland relative to North America: Plate reconstructions of the Davis Strait and Nares Strait regions between Canada and Greenland. *Journal of Geophysical Research Solid Earth*, *117*, B10401.

Peate, I. U., & Bryan, S. E. (2008). Re-evaluating plume-induced uplift in the Emeishan large igneous province. *Nature Geoscience*, *1*(9), 625. https://doi.org/10.1038/ngeo281

Pedersen, V. K., Nielsen, S. B., & Gallagher, K. (2012). The post-orogenic evolution of the Northeast Greenland Caledonides constrained from apatite fission track analysis and inverse geodynamic modelling. *Tectonophysics*, *530*, 318–330. https://doi.org/10.1016/j.tecto.2012.01.018

Piasecki, S., Larsen, L. M., Pedersen, A. K., & Pedersen, G. K. (1992). Palynostratigraphy of the lower Tertiary volcanics and marine clastic sediments in the southern part of the West Greenland Basin: implications for the timing and duration of the volcanism. *Rapport Gronlands Geologiske Under- sogelse*, *154*, 13–31.

Redfield, T. (2010). On apatite fission track dating and the Tertiary evolution of West Greenland topography. *Journal of the Geological Society*, *167*(2), 261–271. https://doi.org/10.1144/0016-76492009-036

Redfield, T. F., Braathen, A., Gabrielsen, R. H., Osmundsen, P. T., Torsvik, T. H., & Andriessen, P. A. M. (2005). Late Mesozoic to early Cenozoic components of vertical separation across the Møre-Trøndelag Fault Complex, Norway. *Tectonophysics*, *395*(3–4), 233–249. https://doi.org/10.1016/j.tecto.2004.09.012

Reiners, P. W., & Farley, K. A. (2001). Influence of crystal size on apatite (U–Th)/He thermochronology: an example from the Bighorn Mountains, Wyoming. *Earth and Planetary Science Letters*, *188*(3–4), 413–420. https://doi.org/10.1016/S0012-821X(01)00341-7

Riis, F. (1996). Quantification of Cenozoic vertical movements of Scandinavia by correlation of morphological surfaces with offshore data. *Global and Planetary Change*, *12*(1), 331–357. https://doi.org/10.1016/0921-8181(95)00027-5

Rohrman, M., & van der Beek, P. (1996). Cenozoic postrift domal uplift of North Atlantic margins: an asthenospheric diapirism model. *Geology*, *24*(10), 901–904. https://doi.org/10.1130/0091-7613(1996)024<0901:CPDUON>2.3.CO;2

Rowberry, M. (2008). Constraining the altitudinal range of sub-horizontaldenudation surfaces in Wales, UK, using the elevation relief ratio. *Revista Geografica Academica*, *2*, 26–40.

Shuster, D. L., Flowers, R. M., & Farley, K. A. (2006). The influence of natural radiation damage on helium diffusion kinetics in apatite. *Earth and Planetary Science Letters*, *249*(3), 148–161. https://doi.org/10.1016/j.epsl.2006.07.028

Spiegel, C., Kohn, B., Belton, D., Berner, Z., & Gleadow, A. (2009). Apatite (U–Th–Sm)/He thermochronology of rapidly cooled samples: the effect of He implantation. *Earth and Planetary Science Letters*, *285*(1), 105–114. https://doi.org/10.1016/j.epsl.2009.05.045

St-Onge, M. R., van Gool, J. A., Garde, A. A., & Scott, D. J. (2009). Correlation of Archaean and Palaeoproterozoic units between northeastern Canada and western Greenland: constraining the pre-collisional upper plate accretionary history of the Trans-Hudson orogen. *Geological Society, London, Special Publications*, *318*(1), 193–235. https://doi.org/10.1144/SP318.7

Strunk, A., Knudsen, M. F., Egholm, D. L., Jansen, J. D., Levy, L. B., Jacobsen, B. H., & Larsen, N. K. (2017). One million years of glaciation and denudation history in west Greenland. *Nature communications*, *8*, 14199. https://doi.org/10.1038/ncomms14199

Thiede, J., Jessen, C., Knutz, P., Kuijpers, A., Mikkelsen, N., Nørgaard-Pedersen, N., & Spielhagen, R. F. (2011). Million years of Greenland Ice Sheet history recorded in ocean sediments. *Polarforschung*, *80*(3), 141–149.

Vermeesch, P., Seward, D., Latkoczy, C., Wipf, M., Günther, D., & Baur, H. (2007). α-Emitting mineral inclusions in apatite, their effect on (U–Th)/He ages, and how to reduce it. *Geochimica et Cosmochimica Acta*, *71*(7), 1737–1746. https://doi.org/10.1016/j.gca.2006.09.020

Wildman, M., Brown, R., Watkins, R., Carter, A., Gleadow, A., & Summerfield, M. (2015). Post break-up tectonic inversion across the southwestern cape of South Africa: New insights from apatite and zircon fission track thermochronometry. *Tectonophysics*, *654*, 30–55. https://doi.org/10.1016/j.tecto.2015.04.012

SUPPORTING INFORMATION

Additional supporting information may be found online in the Supporting Information section at the end of the article.

How to cite this article: Jess S, Stephenson R, Brown R. Evolution of the central West Greenland margin and the Nuussuaq Basin: Localised basin uplift along a stable continental margin proposed from thermochronological data. *Basin Res*. 2018;30:1230–1246. https://doi.org/10.1111/bre.12301